

Nanoscale molecular-switch devices fabricated by imprint lithography

Yong Chen,^{a)} Douglas A. A. Ohlberg, Xuema Li, Duncan R. Stewart,
and R. Stanley Williams

*Quantum Science Research, Hewlett-Packard Laboratories, 1501 Page Mill Road, MS1123, Palo Alto,
California 94304*

Jan O. Jeppesen,^{b)} Kent A. Nielsen,^{b)} and J. Fraser Stoddart

*Department of Chemistry and Biochemistry and The California NanoSystems Institute,
603 Charles E. Young East Drive, University of California, Los Angeles, California 90095-1596*

Deirdre L. Olynick and Erik Anderson

MS 02-400, Lawrence Berkeley National Laboratory, 1 Cyclotron Road, Berkeley, California 94720

(Received 30 August 2002; accepted 16 January 2003)

Nanoscale molecular-electronic devices comprising a single molecular monolayer of bistable [2]rotaxanes sandwiched between two 40-nm metal electrodes were fabricated using imprint lithography. Bistable current–voltage characteristics with high on–off ratios and reversible switching properties were observed. Such devices may function as basic elements for future ultradense electronic circuitry. © 2003 American Institute of Physics. [DOI: 10.1063/1.1559439]

Molecular electronics offers the tantalizing prospect of eventually building circuits with critical dimensions of a few nanometers. Some basic devices utilizing molecules have been demonstrated, including tunnel junctions with negative differential resistance,¹ rectifiers,² and electrically configurable switches that have been used in simple electronic memory and logic circuits.^{3,4} A major challenge that remains is to show that such devices can be fabricated economically using a process that will scale to circuits with large numbers of elements while maintaining their desired electronic properties.

Previous nanoscale molecular devices have been fabricated using e-beam lithography,^{1,4} which is impractical for commercial applications because of the slow writing speed. High-energy electron beams can also damage the active molecules in a circuit. In contrast, imprint lithography is a processing technique that can produce sub-10-nm feature sizes, high throughput, and low cost.⁵ In addition, imprinting may also preclude damage to the active molecules in a circuit from high-energy electrons during e-beam lithography. In this letter, we describe an imprinting process to fabricate nanoscale molecular devices⁶ from an amphiphilic, bistable [2]rotaxane, and demonstrate that these devices act as reversible, electrically toggled switches.

The imprinting mold was fabricated into a 100-nm-thick, thermally grown silicon oxide on a silicon substrate using electron-beam lithography and reactive-ion etching (RIE) with a Leica VB6 electron beam writer and an Oxford Instruments Plasmalab 100 ICP180 RIE. The SiO₂ surface was patterned and etched to leave raised mesas of 40-nm-wide nanowires connected by 3- μ m-wide wires on each end to 100- μ m-square pads. The height of each mesa was 80 nm above the etched surface of the mold. Each mold had 400

such patterns laid out in a geometrical array, to enable a large number of devices to be fabricated with one imprinting step.

To form the device electrodes, a 100-nm-thick polymethylmethacrylate (PMMA) film with a 495 K molecular weight was spin-coated onto a 100-nm-thick SiO₂ layer on a silicon substrate. During imprinting, the mold and polymer-coated device substrate were first heated to 150 °C, which is higher than the glass transition temperature of PMMA (105 °C). The mold was then pressed onto the coated substrate with a homogeneous pressure of 1000 psi to transfer the pattern from the mold into the PMMA layer. The mold and device substrate were then cooled to room temperature before detaching the mold from the PMMA. After imprinting, oxygen RIE was used to remove \sim 10 nm of residual PMMA at the bottom of the imprinted trenches, and expose the SiO₂ surface. Then, 5-nm-titanium (Ti) and 10-nm-platinum (Pt) metal layers were sequentially evaporated onto the substrate. A final acetone lift-off process removed the unpatterned field to leave the Ti/Pt nanowires and their micron-scale connections to the contact pads.

The molecule **R** that we have used in this work is shown in Fig. 1. The **R** label refers to a [2]rotaxane, meaning that the molecule consists of two mechanically interlocked molecular components: a dumbbell encircled by a ring.⁷ A molecular monolayer of the [2]rotaxane **R** was deposited over the entire device substrate, including imprinted bottom metal electrodes, using the Langmuir–Blodgett (LB) method [Fig. 2(a)]. During LB film deposition the aqueous subphase was maintained at pH \sim 8.5 by the addition of tris(hydroxymethyl)aminomethane, to typical concentrations of 10⁻⁴ M, at 21 °C.

Fabrication of the top electrodes began with the blanket evaporation of a 7.5-nm-Ti protective layer. The Ti layer was very reactive with the top functional group of the molecules⁸ to form a direct electrical contact to the molecules, which also blocked the further metal penetration into the LB molecular layers. The Ti layer also minimized subsequent damage to the molecules, enabling further organic resist and sol-

^{a)}Author to whom correspondence should be addressed; electronic mail: yongc@hpl.hp.com

^{b)}Current address: Department of Chemistry, University of Southern Denmark (Odense University), Campusvej 55, DK-5230, Odense M, Denmark.



FIG. 1. (Color) Molecular structure of the bistable [2]rotaxane **R** used to form LB monolayers. The molecule has a hydrophobic (dark green) and a hydrophilic (light blue) stopper. The [2]rotaxane has cyclobis(paraquat-*p*-phenylene) (dark blue) as the ring component and the supporting counterions are hexafluorophosphate.

vent processing [Fig. 2(b)]. Patterned top electrodes of 5-nm Ti and then 10-nm Pt were next fabricated with the same imprinting process just described, using the same mold. For the top electrodes, the imprinting mold was oriented perpendicular to the bottom electrodes and aligned to ensure that the top and bottom nanowires crossed [Fig. 2(c)]. Previous experiments indicated that the [2]rotaxane molecules remained stable up to $\sim 210^\circ\text{C}$,⁹ therefore, the molecular structure should not be changed during the imprinting process. Finally, RIE with CF_4 and O_2 (4:1) gases at a pressure of 40 mTorr and a power of 200 W was used to remove the blanket Ti protective layer anisotropically down to the SiO_2

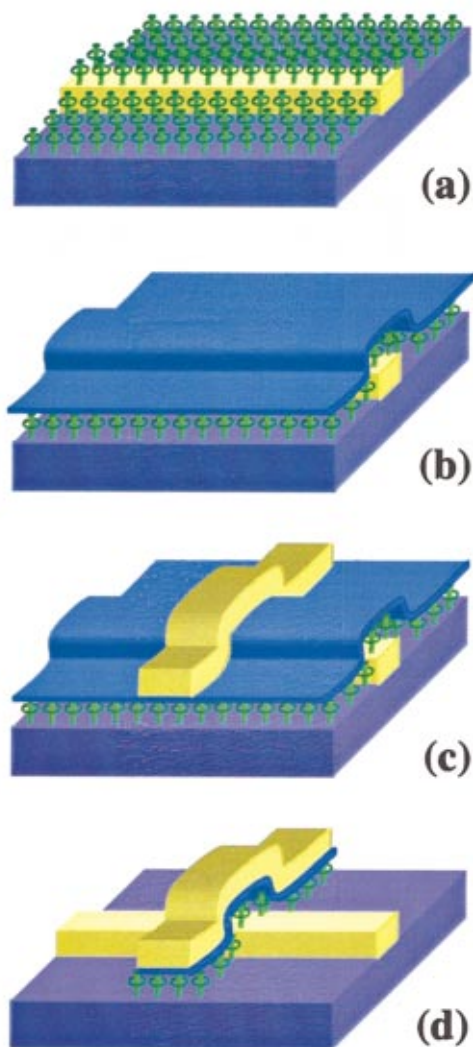


FIG. 2. (Color) Schematic of the procedure used for fabrication of nanoscale molecular-switch devices by imprint lithography.

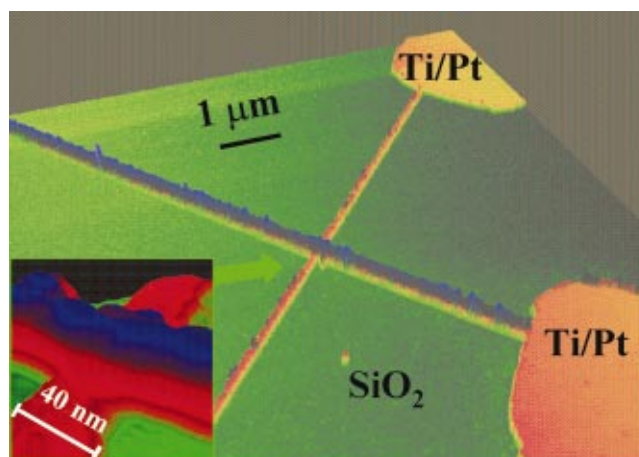


FIG. 3. (Color) An atomic force micrograph of a nanoscale cross-point molecular device with an insert showing the details of the cross point.

layer, but selectively leave the Pt electrodes intact. The molecules and Ti layer under the Pt top electrode were protected. After RIE, an array of devices with the molecular monolayer sandwiched between two metal nanowires remained [Fig. 2(d)].

An atomic force microscope (AFM) image of a cross-point molecular device fabricated with our imprint lithography process is shown in Fig. 3. In order to achieve nanometer lateral resolution, a carbon nanotube tip (ProbeMax) was used as the AFM probe. Only the region near the active part of the device, comprising the two crossed nanowires and their connections to the microscale wires, is shown in the images. The nanowires have a measured width of ~ 40 nm, which is consistent with the 40-nm width of the nanowire templates in the mold. A high-resolution image of the crossed electrodes [Fig. 3 (inset)] shows the active junction area of $\sim 40\text{ nm} \times 40\text{ nm}$.

Ellipsometric analysis of the [2]rotaxane monolayers yielded an average film thickness of 3.5 nm. A static water contact angle of $\sim 90^\circ$ indicated a hydrophobic surface and thus dense monolayer coverage. The active device area of 1600 nm^2 corresponds to ~ 1100 molecules sandwiched between the two electrodes, as determined from the known density of molecules on the surface of the Langmuir trough before transfer to the substrate. In previous studies utilizing silicon bottom and titanium top electrodes, switchable bistable current-voltage characteristics were observed in both microscale and nanoscale devices with the same [2]rotaxane **R** monolayer.⁴ In our lab, microscale devices with this molecule sandwiched between titanium top and platinum bottom electrodes exhibited switching and continuously tunable resistance over a 10^2 – $10^5\ \Omega$ range under current or voltage control.¹⁰

The devices were tested electrically at room temperature under ambient conditions with direct I – V sweeps using a HP 4155A semiconductor parameter analyzer and a KarlSuss PSM6 probe station. The measured resistances of the Ti/Pt nanowires varied in the range from 17 to 25 k Ω , determined by two-terminal measurements across a single wire. The nanowire resistances and the probe/metal contacts ($< 50\ \Omega$) were still significantly smaller than the molecular

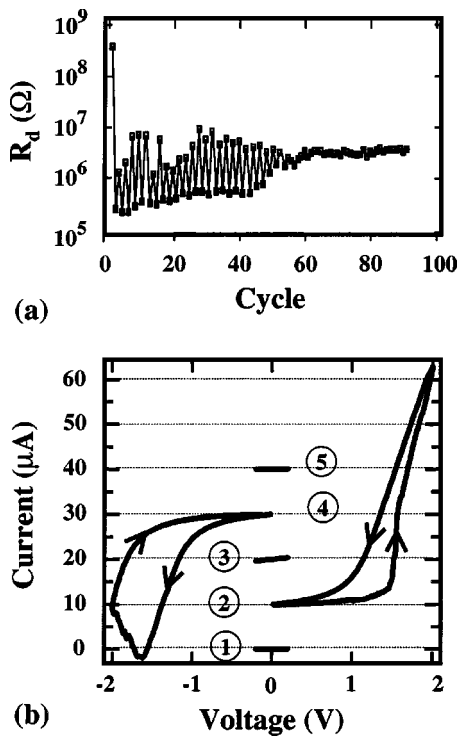


FIG. 4. Electronic characteristic of a nanoscale molecular device. (a) The resistances of the device (R_d) recorded (read) at 0.2 V after multiple switching cycles with the open (filled) squares representing R_d measured after a negative (positive) writing voltage cycle applied to the device. (b) I - V curves showing a complete off-on-off device switching cycle. Curves 1-5 are offset by 20 μA from each other for clarity.

monolayer resistance, and they have been neglected in the subsequent device measurements.

Current-voltage characteristics of the molecular monolayer devices were obtained by applying a test voltage (V_T) to the top electrode while grounding the bottom electrode. As fabricated, the molecular devices usually showed a very high resistance, $>10^8 \Omega$, when measured at $V_T=0.2$ V. This initial high resistance state was stable for $|V_T|<2$ V. Exceeding these voltage limits usually caused an irreversible transition to a smaller resistance. For example, the initial resistance of a typical device measured at 0.2 V was $6.1 \times 10^8 \Omega$, shown as the first point in Fig. 4(a). After sweeping the voltage bias cycle from 0 to +5 V, the resistance subsequently measured at 0.2 V dropped to $4.3 \times 10^5 \Omega$. After this "burn-in" step, similar to that reported for our microscale devices,¹⁰ the nanoscale molecular devices became reversible switches with lower cycling voltages from 0 to ± 2 V. A typical switching cycle is shown in Fig. 4(b) for the same device shown in Fig. 4(a). To compare the resistances after each writing process, the resistance for a device (R_d) was always measured (read) at 0.2 V. After the initial burn-in, the molecular device was set in the "off" state, the I - V characteristic measured in the range ± 0.2 V showed an ohmic response [curve 1 in Fig. 4(b)] with $R_d=8.1 \times 10^6 \Omega$. A positive voltage bias cycle between 0 to 2 V was next applied to the device, and yielded a counterclockwise I - V hysteresis loop [curve 2 in Fig. 4(b)]. In this "on" state, the resistance was $R_d=4.8 \times 10^5 \Omega$ [curve 3 in Fig. 4(b)]. A subsequent

negative voltage bias cycle from 0 to -2 V was then applied to the device, yielding a clockwise I - V hysteresis [curve 4 in Fig. 4(b)]. The device was again in the off state, with $R_d=9.2 \times 10^6 \Omega$ [curve 5 in Fig. 4(b)]. Figure 4(a) shows the evolution of the measured resistance R_d through 95 repetitions of this switching cycle. The on/off switching events were repeatable, as shown in Fig. 4(a). However, the on/off ratio of R_d for this device decreased gradually after ~ 40 switch cycles.

Statistically, $\sim 75\%$ of the 36 devices we tested showed such reversible switching properties. The rest of the devices were either "shorted" (with their resistances $<10^5 \Omega$ (comparable to the nanowire resistance), or "open," with resistances $>10^8 \Omega$ that remained unchanged even after a high burn-in voltage (>8 V) was applied. The open devices included some with structural defects, such as broken nanowires, detected by post-measurement scanning electron microscopy (SEM). However, some "defect-free" devices as determined by SEM still had an open electrical character, perhaps due to a contact problem between the metal electrodes and molecular monolayer. For a device that switched reversibly, the positive threshold voltage to turn it on ranged from 0.5 V to 3 V; the negative threshold voltage to switch it off ranged from -0.5 to -3.5 V. Any voltage bias $|V|<0.5$ V applied to the devices did not change their resistance state. Both the positive and negative switch threshold voltages varied between devices, and from one switch cycle to another for a given device. A voltage bias $V>|3$ V caused some devices to irreversibly short. At the beginning of switch cycling, the on/off resistance ratios ranged from 2 to 10^4 for different devices. The ratio typically decayed below 2 and gradually approached 1 after a few to several hundred cycles for different devices; several devices measured after an interval of two months retained the resistance of the state into which they had last been set.

The authors gratefully acknowledge H. Wiersma, T. Ha, P. Beck, and S.-H. Leung for experimental assistance, T. I. Kamins, P. J. Kuekes, Y. Luo, C. P. Collier, and J. R. Heath for valuable discussions, and the Defense Advanced Research Projects Agency in the United States and by the Carlsbergfondet in Denmark for partial support.

¹J. Chen, M. A. Reed, A. M. Rawlett, and J. M. Tour, *Science* **286**, 1550 (1999).

²R. M. Metzger, *Acc. Chem. Res.* **32**, 950 (1999).

³C. P. Collier, E. W. Wong, M. Belohradský, F. M. Raymo, J. F. Stoddart, P. J. Kuekes, R. S. Williams, and J. R. Heath, *Science* **285**, 391 (1999).

⁴Y. Luo, C. P. Collier, J. O. Jeppesen, K. A. Nielsen, E. Delonno, G. Ho, J. Perkins, H. Tseng, T. Yamamoto, J. F. Stoddart, and J. R. Heath, *Chem. Phys. Chem.* **3**, 519 (2002).

⁵S. Y. Chou, P. R. Krauss, and P. J. Renstrom, *Science* **272**, 85 (1996).

⁶Y. Chen, in U.S. Patent No. 6,432,740 (2002).

⁷A. R. Pease, J. O. Jeppesen, J. F. Stoddart, Y. Luo, C. P. Collier, and J. R. Heath, *Acc. Chem. Res.* **34**, 433 (2001).

⁸K. Konstadinidis, P. Zhang, R. L. Opila, and D. L. Allara, *Surf. Sci.* **338**, 300 (1995).

⁹J. O. Jeppesen, K. A. Nielsen, J. Perkins, S. A. Vignon, A. D. Fabio, R. Ballardini, M. T. Gandolfi, M. Venturi, V. Balzani, J. Becher, and J. F. Stoddart (unpublished).

¹⁰D. R. Stewart, D. A. A. Ohlberg, P. Beck, Y. Chen, R. S. Williams, J. O. Jeppesen, K. A. Nielsen, and J. F. Stoddart, *Appl. Phys. Lett.* (in press).